

NON-INVASIVE ANGIOGRAPHY

Core Curriculum

Applications of Multislice Coronary Computed Tomographic Angiography to Percutaneous Coronary Intervention: How Did We Ever Do Without It?

Harvey S. Hecht,* MD, FACC

By providing data previously available only by intravascular ultrasound, 64-slice multidetector computed tomographic angiography (CTA) will impact percutaneous coronary intervention (PCI) in multiple areas: (1) pre-PCI patient selection; (2) identification of significant lesions; (3) in-stent restenosis; (4) procedure planning: stent sizing, choice of intervention, and equipment, chronic total occlusions, 3D-CTA in the catheterization laboratory; (5) plaque evaluation and identification of high-risk lesions; (6) postcatheterization decisions, and (7) structural heart disease. The likely outcome is transformation of the catheterization laboratory into a streamlined interventional suite, utilizing on-line CTA data in an interactive format. © 2008 Wiley-Liss, Inc.

Key words: imaging (CT/MR); percutaneous coronary intervention; quantitative coronary angiography

The introduction of 64-slice multidetector computed tomographic coronary angiography (CTA) heralds a new era in percutaneous coronary intervention (PCI). By combining the best characteristics of catheter angiography (CA) while avoiding its pitfalls, with data previously available only with intravascular ultrasound (IVUS), CTA impacts multiple facets of PCI, the most important of which are listed in Table I. In multiple areas, tomographic intravascular analysis (TIVA) facilitates decision making by providing data unobtainable from CA.

PRE-PCI PATIENT SELECTION

The traditional patient evaluation paradigm employs nuclear or echocardiographic stress testing to identify patients who are candidates for PCI by demonstrating sufficient myocardium at jeopardy to warrant intervention. The sensitivities and specificities for these modalities (86 and 67% for nuclear and 85 and 75% for stress echo [1]) are considerably less than for 64-slice CTA (90 and 95%, respectively [2]), suggesting that CTA is the preferred first test. Moreover, nuclear, in particular, is problematic in those situations where accurate evaluation is most important: 40% of patients with triple vessel disease will have normal (12%) or

low-risk single vessel ischemia images (28%) [3]. In patients with left main disease, 15% will have normal (10%) or low-risk (5%) studies [4]. Stress testing may be performed after CTA to determine the functional significance of 50–75% stenoses demonstrated on CTA, in which case significant ischemia would justify PCI, and the absence thereof would suggest medical treatment. CTA revealing <50% or >75% stenoses do not require stress testing validation, since a positive stress test with a <50% stenosis is, by definition, a false positive, and a negative test with a >75% stenosis is a false negative.

Department of International Cardiology, Lenox Hill Heart and Vascular Institute, New York, New York

Grant sponsor: Philips Medical Systems.

*Correspondence to: Harvey S. Hecht, Lenox Hill Heart and Vascular Institute, 130 E. 77th St., New York, NY 10021.
E-mail: hhecht@aol.com

Received 30 September 2007; Revision accepted 3 October 2007

DOI 10.1002/ccd.21427

Published online 25 February 2008 in Wiley InterScience (www.interscience.wiley.com).

IDENTIFICATION OF SIGNIFICANT LESIONS

Since its inception, CA has relied upon percent diameter stenosis (%DS) derived from minimum luminal diameters (MLD) as the primary decision making tool. IVUS [5–8] and fractional flow reserve (FFR) [6,8–11] are more recent developments that provide more objective measurements of stenosis significance; IVUS yields minimum luminal area (MLA), which is directly related to flow even though it is not directly

measuring flow. MLD has no bearing on flow unless the lesion is absolutely concentric; it simply represents the narrowest presentation of the stenosis obtained during the CA. FFR determines the physiological significance of a stenosis by measuring flow limitation across a single vascular bed in response to adenosine. Both techniques have been validated by nuclear imaging and correlate well with each other, despite the common belief that IVUS promotes, and FFR avoids, PCI. Conventional IVUS criteria for defining significant stenoses are MLA $<4.0 \text{ mm}^2$ for proximal vessels, and $<6.0 \text{ mm}^2$ for the left main coronary artery [11]. FFR <0.75 is considered diagnostic of significant stenosis [11].

CTA, by imaging the vessel wall as well as the lumen from a 360° perspective, offers distinct advantages compared to CA despite the superior temporal and spatial resolution of CA (5–10 msec and 200μ , respectively) compared to CTA (50–200 msec and 350μ , respectively).

1. Insufficient sampling error: The 360° perspective provides an infinite number of viewing angles to

TABLE I. PCI Areas of CTA Impact

Pre PCI patient selection
Identification of significant lesions
In-stent restenosis
Procedure planning
(a) stent sizing
(b) chronic total occlusions
(c) 3DCTA in the catheterization laboratory
Plaque evaluation and identification of high risk lesions
Postcatheterization decisions
Structural heart disease

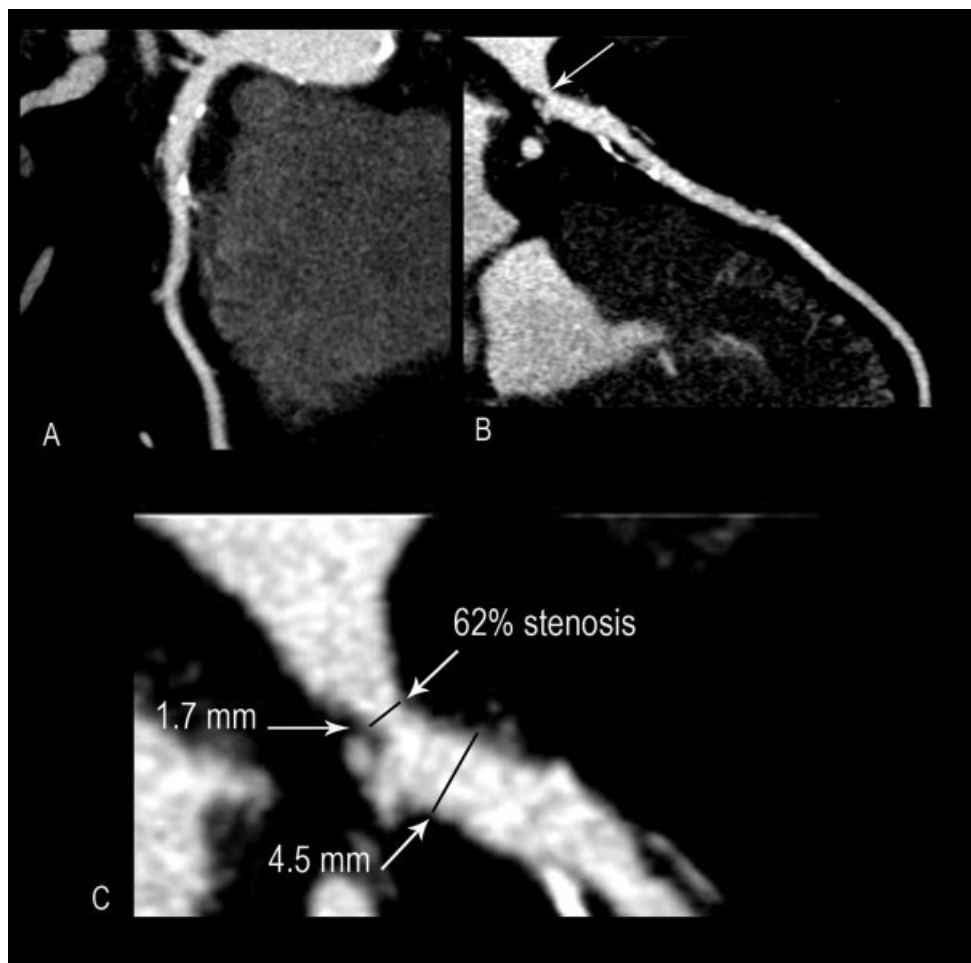


Fig. 1. A 76-year-old man presented with exertional dyspnea. (A) Left anterior oblique and (B) right anterior oblique CTA curved multiplanar reconstruction of the left anterior descending coronary artery demonstrated a significant stenosis apparent only in (B). Quantitative measurement of the stenotic area is shown in (C). Abbreviation: CTA, computed tomographic angiography.

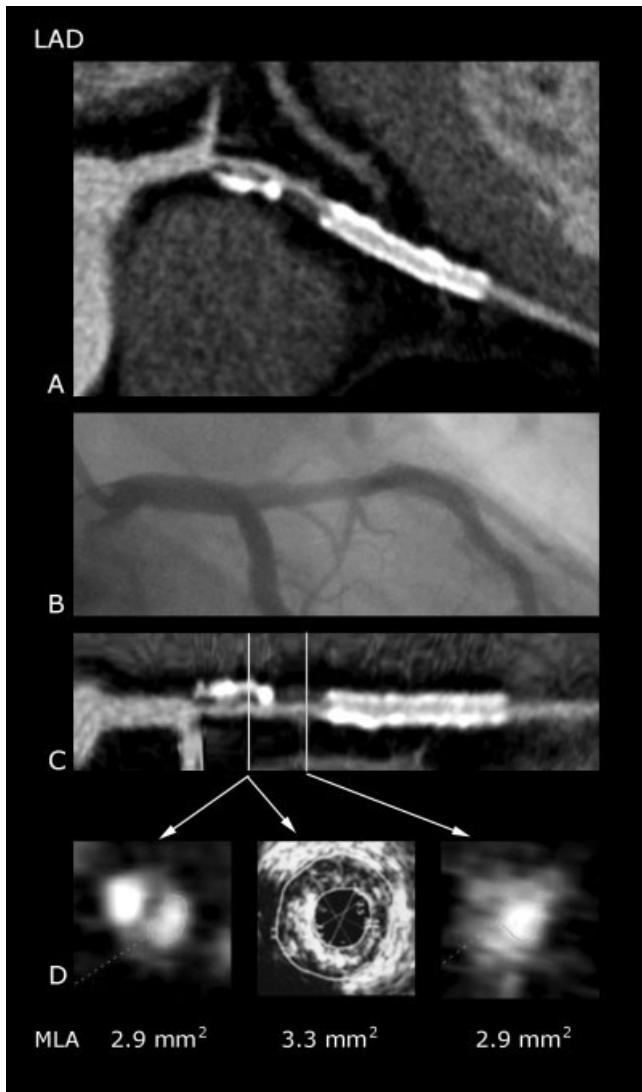


Fig. 2. In a symptomatic 64-year-old male with prior LAD stent, CTA curved MPR of the LAD (A) revealed significant diffuse narrowing from the LAD ostium to the stent, with only mild narrowing evident on the corresponding CA (B). TIVA (D) of the straightened MPR (C) demonstrated significantly reduced MLA of 2.9 mm², confirmed by IVUS (D), and followed by PCI. Abbreviations: CA, catheter angiography; LAD, left anterior descending; CTA, computed tomographic angiography; MLA, minimum luminal area; MPR, multiplanar reconstruction; PCI, percutaneous coronary intervention; TIVA, tomographic intravascular analysis.

ensure capturing the stenosis in its narrowest dimension, compared to the insufficient sampling error inherent in the limited number of acquisitions of CA (6–7 for the left and 2–4 for the right coronary arteries).

2. **Overlap:** Overlapping vessels, which frequently complicate CA, are never an issue for CTA; each vessel is tracked independently.
3. **Foreshortening:** The least foreshortened view of each vessel is readily determined by available algorithms.

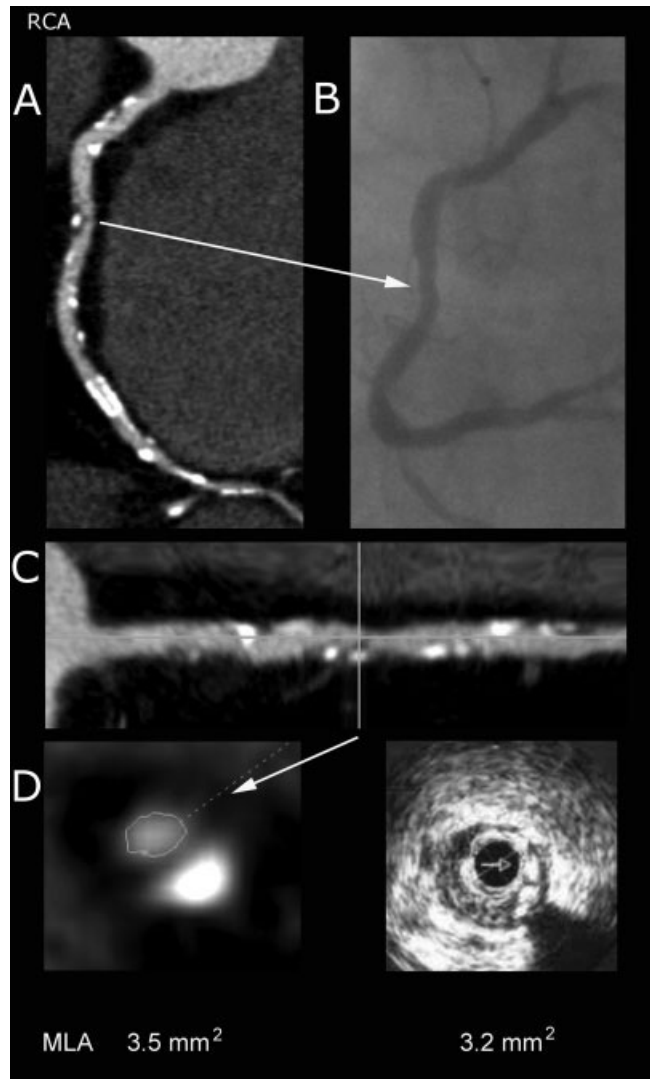


Fig. 3. A 56-year-old female with angina presented to the emergency room. CTA curved MPR revealed severe mid RCA stenosis (A) not apparent on subsequent CA (B). TIVA (D) of the straightened MPR (C) demonstrated significantly reduced MLA of 3.5 mm², confirmed by IVUS (D), and followed by PCI of the affected area. Abbreviations: CA; catheter angiography; CTA, computed tomographic angiography; MLA, minimum luminal area; MPR, multiplanar reconstruction; PCI, percutaneous coronary intervention; RCA, right coronary artery; TIVA, tomographic intravascular analysis.

4. **Remodeling and reference areas:** Accurate calculation of %DS is predicated on identification of appropriate proximal and distal reference areas, a task complicated by the inability of CA to identify areas of positive and negative remodeling. CTA is ideally suited for this purpose and remodeling index is an easily measurable parameter [12], thereby facilitating appropriate choice of reference areas. Quantitative CTA (QCTA) should always be employed (Fig. 1); “eyeballing”, with its inherent overestima-

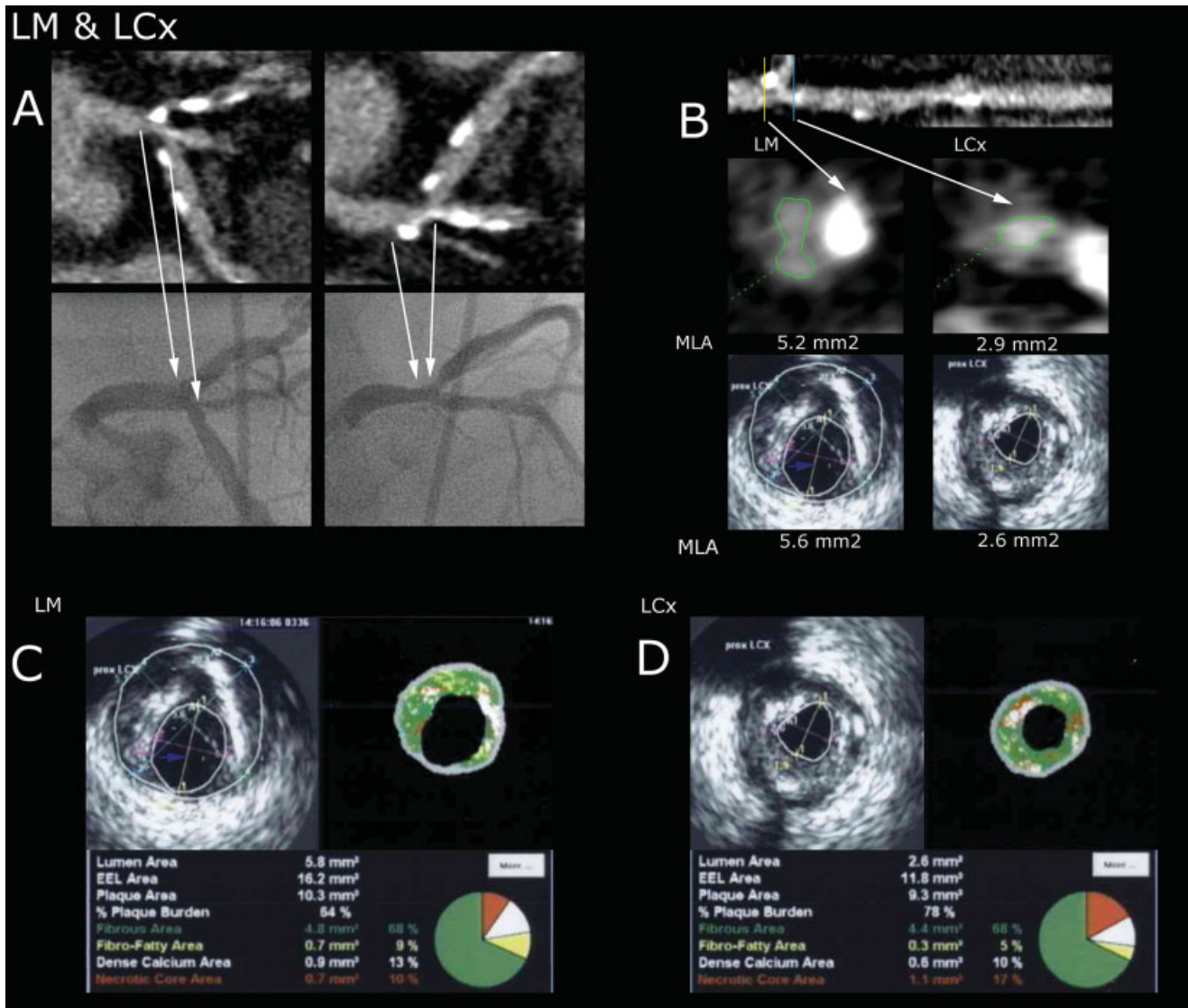


Fig. 4. In a 60-year-old female with exertional dyspnea, CTA curved MPR demonstrated significant LM and ostial LCx disease less apparent on the subsequent CA (A). TIVA of the straightened MPR (B) demonstrated significantly reduced LM MLA of 5.2 and 2.9 mm² for the LCx, confirmed by IVUS (B), and followed by bypass surgery. Virtual histology revealed predominantly fibrous plaque in the LM (C) and LCx (D), with a

slightly increased necrotic core (17%) in the LCx. Abbreviations: CA, catheter angiography; CTA, computed tomographic angiography; LCx, left circumflex coronary artery; LM, left main coronary artery; MLA, minimum luminal area; MPR, multiplanar reconstruction; TIVA, tomographic intravascular analysis. [Color figure can be viewed in the online issue, which is available at www.interscience.wiley.com.]

tion, is not an acceptable method of analysis, despite being the standard of care for CA.

5. MLA calculation: As noted earlier, MLA is a far more important physiologic parameter than MLD, and can be reliably derived by tomographic intravascular analysis (TIVA) of cross-sectional images, with correlation with IVUS measurements (Figs. 2–4, 7, 9, 15) [13,14]. MLA cannot be derived from CA.
6. Diffuse narrowing: Segments with relatively uniform diffuse lumen reduction will be angiographically inapparent on CA since there is no appropriate reference

point, and MLA calculations are not available. The absence of a reference area is not problematic for CTA since the MLA can be determined (Fig. 2).

Consequently, a CTA-guided PCI paradigm has been developed (Fig. 5) [2] in which CTA rather than stress testing is the first step in patient evaluation. Benign CTA diameter and area measurements triage the patient to medical management. Patients with severe disease, defined as >75% stenosis, progress directly to CA. These patients are relatively few in number, since

CTA Guided PCI Paradigm

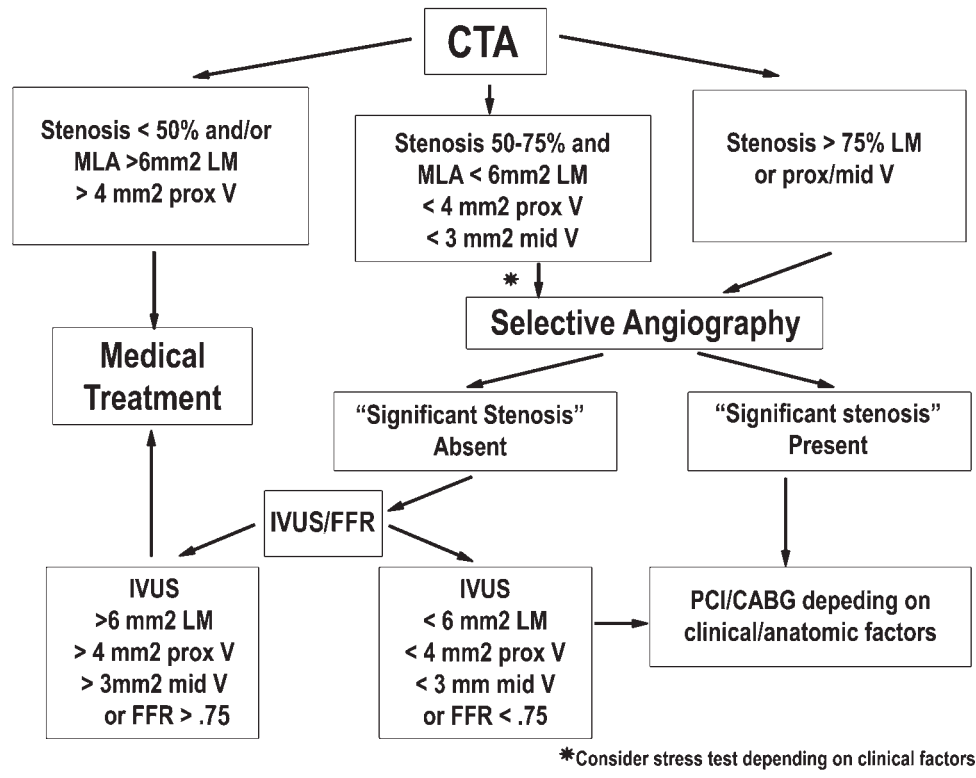


Fig. 5. CTA guided PCI paradigm. Abbreviations: CABG, coronary artery bypass grafting; CTA, computed tomographic angiography; FFR, fractional flow reserve; IVUS, intravascular ultrasound; LM, left main; MLA, minimum lumen area; PCI, percutaneous coronary intervention; V, vessel.

TABLE II. 64-Slice Computed Tomographic Angiography Detection of In-Stent Restenosis

Study	Patients (N)	Stents (N)	% with ISR	Sens (%)	Spec (%)	PPV (%)	NPV (%)	UE	Scanner
Rixe [15]	65	59	11.9	86	98	86	98	42%	Siemens
Cademartiri [16]	182	178	11.8	50	57	13	89	UEI	Toshiba/Siemens
	192		10.9	91	86	42	99	UEI	
Ehara [17]	71	115	19.1	91	93	77	98	12%	Siemens
	81	125	19.2	92	81	54	98	UEI	
Hecht [18]	67	136	12.5	94	74	39	99	0%	Philips

Abbreviations: ISR, in-stent restenosis; N, number; UE, unevaluable stents; UEI, unevaluable stents included; NPV, negative predictive value; PPV, positive predictive value; Sens, sensitivity; Spec, specificity.

QCTA excludes positively remodeled reference areas and avoids the overestimation of “eyeballing” lesions. Similarly >75% stenoses are infrequently noted on CA when quantitative analysis, rather than visual estimation, is employed.

Stenoses from 50–75% which fulfill the IVUS MLA criteria derived from the TIVA may be evaluated by stress testing to determine their functional significance; a positive test will lead to CA, and a negative test to medical management. However, keeping in mind the limitations of myocardial perfusion imaging in left main and triple vessel disease, CA may immediately

follow the CTA without intervening stress evaluation. Stenoses (50–75%) which do not fulfill the IVUS MLA criteria do not warrant further evaluation or intervention.

Demonstration of significant disease by CA will lead to PCI. If significant stenosis is not angiographically apparent, IVUS or FFR should be done, with subsequent PCI (Figs. 2, 3, 7, 9, 14) or bypass surgery (Figs. 4, 11) depending on the result. In this large patient subset, the ultimate decision is based upon the CTA-guided IVUS or FFR, and not simply on the CTA alone. This CTA-guided PCI paradigm is depend-

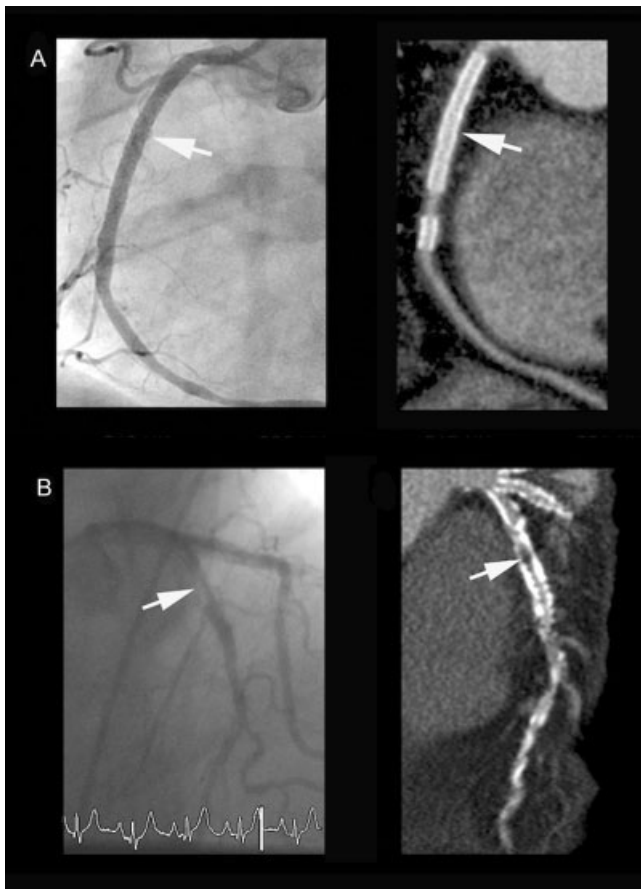


Fig. 6. Normal patent proximal and mid right coronary artery stents (arrows) seen on CA (A, left) and CTA curved MPR (A, right). (B) Severe in-stent restenosis (arrows) in a proximal LAD stent seen on CA (left). Severe hypodensity within the stent is evident on the CTA curved MPR (right). PCI was performed. Abbreviations: CA, catheter angiography; CTA, computed tomographic angiography; MPR, multiplanar reconstruction; PCI, percutaneous coronary intervention.

ent on the ability of each laboratory to document the accuracy of their MLA measurements by IVUS correlations.

IN-STENT RESTENOSIS

There have been several studies evaluating the ability of 64-slice CTA to detect in-stent restenosis (ISR) (Table II) [15–18]. The low frequency of ISR results in poor predictive accuracy, despite the superb sensitivity and reasonable specificity. Artifact from stent material and superimposed calcification may render interpretation difficult. Nonetheless, while stent evaluation is not an approved CTA indication [19], the excellent negative predictive accuracy and sensitivity have lead to its routine use in many centers. Restriction to patients with a higher pretest likelihood of ISR based upon recurrence of symptoms will lead to a higher

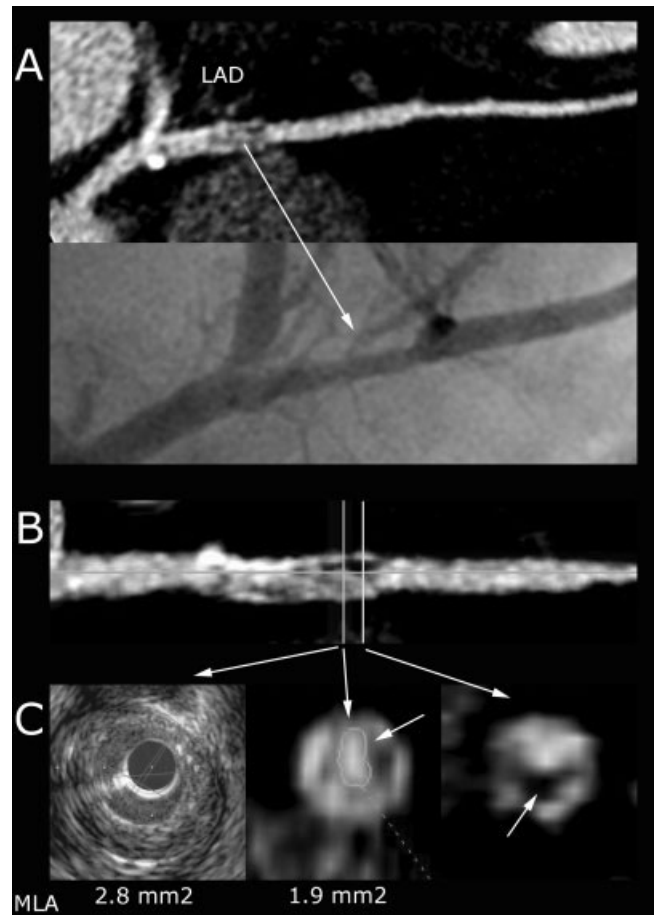


Fig. 7. An 80-year-old female with increasing dyspnea and prior LAD stenting was evaluated. CTA revealed severe hypodensity consistent with significant in-stent restenosis (A, top) that appeared to be only moderately severe on CA (A, bottom). TIVA (C) of the straightened MPR (B) in two adjacent areas of the stent demonstrated the hypodensity characteristic of neointimal hyperplasia (arrows), as well as severely decreased MLA, confirmed by IVUS (C). PCI was performed. In-stent MLA calculation is rarely possible. Blooming artifact from the dense stent material almost always precludes accurate measurement; ISR is diagnosed by qualitative density levels. Abbreviations: CA, catheter angiography; CTA, computed tomographic angiography; IVUS, intravascular ultrasound; LAD, left anterior descending; MLA, minimum lumen area; MPR, multiplanar reconstruction; TIVA, tomographic intravascular analysis.

positive predictive accuracy. Examples of normal stents and ISR are shown in Figs. 6–8.

PROCEDURE PLANNING

Stent Sizing

While accurate longitudinal and axial stent sizing has always been important, the great majority of stents are implanted solely on the basis of visual assessment at the time of the procedure, without the benefit of

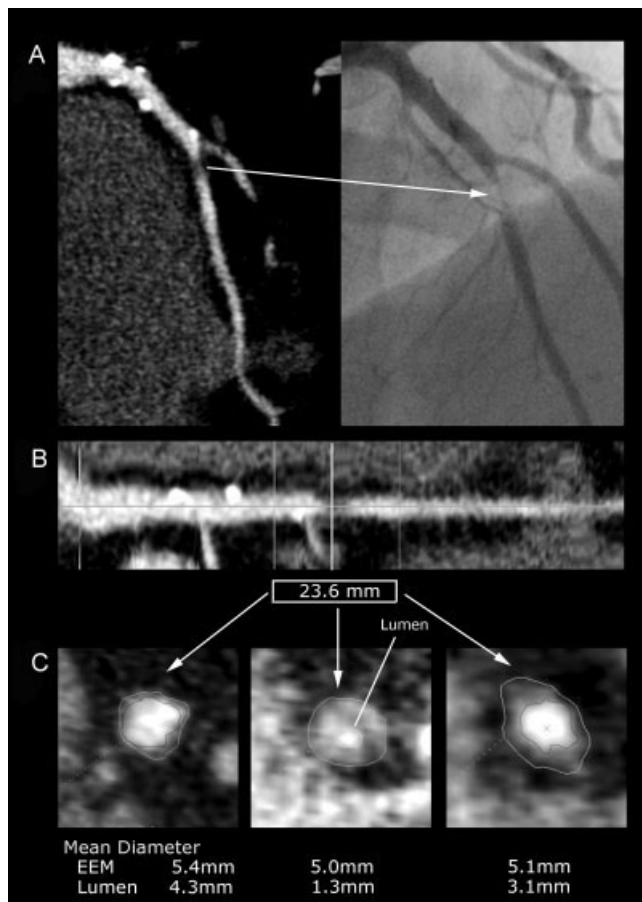


Fig. 8. In a 66-year-old male with increasing angina, subtotal LAD occlusion (arrow) was noted on the CTA (A, left) and on the CA (A right). Proximal and distal stent landing zones, 23.6 mm apart, were chosen on the straightened MPR (B). Mean luminal diameters for the landing zones were determined by TIVA to be 4.4 mm and 3.4 mm, respectively (C). PCI was performed using a 25 mm × 3.5 mm stent, with postinflation of the proximal segment to 4.5 mm to achieve full apposition. Abbreviations: CA, catheter angiography; CTA, computed tomographic angiography; IVUS, intravascular ultrasound; LAD, left anterior descending; MPR, multiplanar reconstruction; PCI, percutaneous coronary intervention; TIVA, tomographic intravascular analysis.

objective IVUS measurements. More recently, concerns about late stent thrombosis [20] have heightened awareness of the need for accurate stent sizing since an IVUS-directed change from 3.0 mm to 3.5 mm in diameter may convert a stent from drug eluting to bare metal, with similar ISR outcomes, lower risk of late stent thrombosis, and shorter duration of clopidogrel therapy. Longitudinal stent deployment may be affected by a more in-depth assessment of the area to be covered; areas of significant disease not apparent by conventional angiography may be included (Fig. 8).

Choice of Intervention and Equipment

A clearer delineation of the path traversed en route to the target lesion and of the lesion area itself may alter the treatment plan. Ostial left anterior descending disease may be better treated by bypass surgery if CTA demonstrates more left main disease than is apparent angiographically; PCI in these circumstances may traumatize the left main and lead to significant left main stenosis (Fig. 9). Calcification is always more visible on CTA than on CA, and, if extensive, may convert a planned straightforward stent placement to a rotoblator or surgical procedure. Extensive low-density lipid laden plaque proximal to the target zone may alert the operator to possible catheter-induced embolization of friable tissue. CTA analysis of the size and angulation of the aortic root and ostial location may facilitate correct guiding catheter choice.

Chronic Total Occlusions

The use of CTA to predict successful intervention for chronic total occlusions (CTO) has been previously described [21]. More importantly, CTA can be utilized to directly guide the procedure in the catheterization laboratory. While segments of the totally occluded vessel may not be visualized by CA, they are always apparent on CTA, and their visualization will facilitate passage of the guide wire. In particular, attempted opening of flush occlusions may result in fruitless attempts to locate the entrance to the CTO without the guidance provided by CTA mapping (Fig. 10).

3DCTA in the Catheterization Laboratory

CTA can be imported directly to the catheterization laboratory monitor and electronically linked to the C-arm, which can then be rotated, with accompanying automatic rotation of the CTA map to the angle with the least foreshortening and overlap of the target area as determined by the CTA. This should enable more accurate longitudinal stent sizing than would be feasible from unknowingly foreshortened CA views. Stent placement would be facilitated as well by decreasing the number of CA images that would otherwise be needed to acquire less foreshortened and overlapped images; imaging in the catheterization laboratory can begin with the best angle preselected from the 3DCTA map. As noted earlier, flush occluded CTOs are ideal beneficiaries of 3DCTA mapping (Fig. 10). A randomized controlled trial comparing 3DCTA guided PCI to conventional PCI is in progress.

PLAQUE EVALUATION AND IDENTIFICATION OF HIGH-RISK LESIONS

CTA plaque evaluation is dependent on density measurements, using X-ray attenuation defined by Hounsfield units (HU). Lipid is defined as tissue with an HU range of 0 to -150, noncalcified plaque from 0

to 130 with values increasing as the content increases from fat to fibrous tissue, and calcified plaque as >130 HU. Contrast ranges in density, depending on the degree of dilution and the size of the patient; typically, it ranges from 250 to 500 HU in proximal vessels. However, these values are relevant only in vitro; in the real world of in vivo imaging, apparent tissue density is profoundly affected by the “company it keeps”.

Volume averaging, or the partial volume effect, will increase the HU of low-density tissue that is adjacent to denser material (e.g., contrast, calcified plaque) by sharing voxels with the higher density tissue, with a resultant increase in the average HU of the sample. Thus, lipid measuring -50 HU in vitro, may measure 100 HU next to a 500 HU calcified plaque, and will no longer be classified as lipid. At the other extreme, “beam hardening”, manifested by extremely dense material blocking photons from reaching adjacent tissue, may transform contrast with an in vitro HU of 350 to the negative density of lipid (0 to -150), if it is adjacent to a densely calcified plaque (HU > 1,000), and would lead to an erroneous classification. There is currently no acceptable solution; absolute HU cannot be used for plaque characterization across the wide variety of complex plaque typically encountered in the average diseased vessel. Algorithms employing HU gradients between adjacent structures are under evalua-

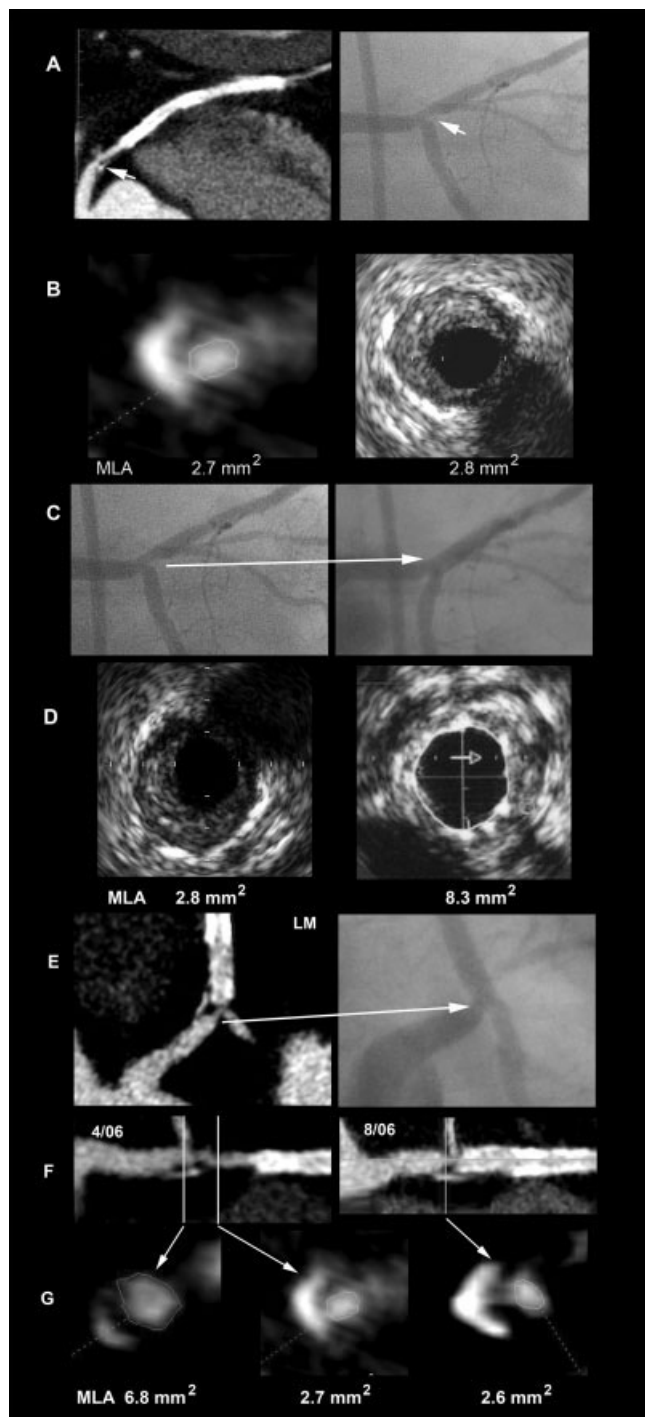


Fig. 9. A proximal LAD stent was implanted in a 56-year-old male who presented with angina. Five months later, symptoms recurred and CTA revealed severe ostial stenosis (A, left) that was angiographically inapparent (A, right). TIVA yielded an ostial MLA of 2.7 mm² (B, left), leading to IVUS evaluation which confirmed the TIVA findings (B, right). Ostial stenting was performed, with angiographic improvement (C) and increase of the MLA from 2.8 to 8.3 mm² (D). The operator was aware of the moderate distal LM disease noted on the CTA prior to the procedure (G, left) and confirmed by IVUS, but the small caliber distal vessel prompted PCI rather than CABG. Symptoms disappeared but returned after 4 months; CTA demonstrated critical left main stenosis and patency of the LAD stent (E, left), confirmed by CA (E, right); CABG was performed. Comparison of the LM and ostial LAD TIVA (F, G) from the two evaluations documented a decrease of the LM MLA from 6.7 to 2.6 mm², and patency of the ostial stent (G). Trauma from the PCI undoubtedly led to the LM disease; similar insult to the ostial LAD during the first stent implantation was the likely etiology of the ostial disease, which was angiographically inapparent. CTA provides the operator with an analysis of the vessel en route to the target lesion, revealing disease that may not be obvious on CA, and potentially altering the choice of procedure. Abbreviations: CA, catheter angiography; CABG, coronary artery bypass grafting; LAD, left anterior descending; CTA, computed tomographic angiography; MLA, minimum luminal area; MPR, multiplanar reconstruction; PCI, percutaneous coronary intervention; TIVA, tomographic intravascular analysis.

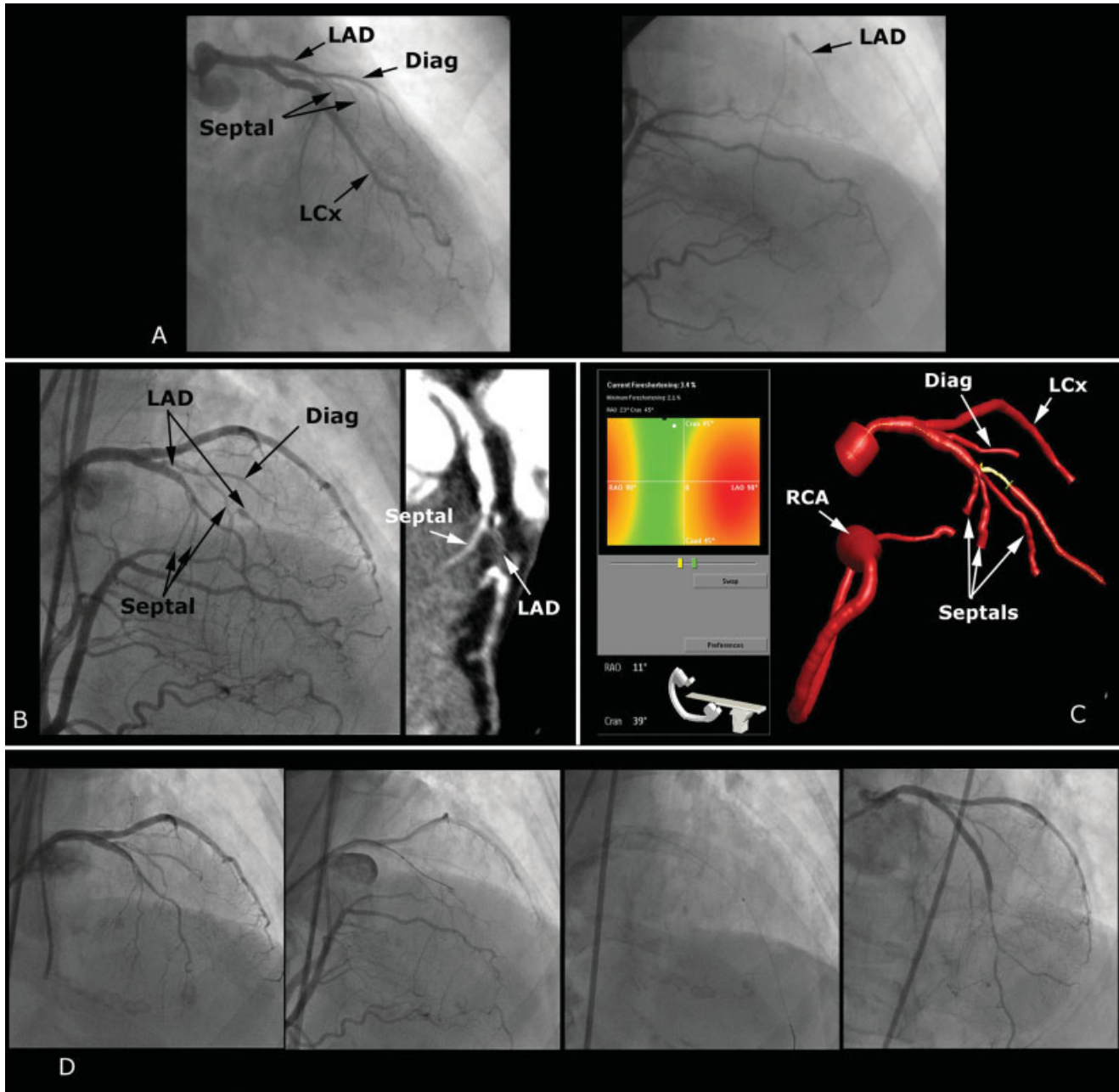


Fig. 10. Selective angiography demonstrated flush occlusion of the LAD with partial collateral filling from the RCA (A) in a symptomatic 65-year-old woman with anterior ischemia. After 6 months of persistent symptoms, CTA guided intervention was planned. Curved MPR readily visualized the occluded LAD segment (B right). CTA mapping (TrueView, Philips Medical Systems) of the left coronary artery and all its branches (C) was imported to the catheterization laboratory monitor and electronically linked to the C-arm. The C-arm was rotated, with accompanying automatic rotation of the TrueView map to the angle predetermined by the CTA to best demonstrate the

origin and course of the chronic total occlusion without overlapping branches. Simultaneous injection of the right and left coronary arteries (B left) was performed. With TrueView guidance, the guidewire was introduced to the precise origin of the flush occlusion, followed by successful recanalization and further stenting of the distal vessel 6 weeks later (D). Abbreviations: CTA, computed tomographic angiography; diag, diagonal; LAD, left anterior descending; LCx, left circumflex; MPR, multiplanar reconstruction; RCA, right coronary artery. [Color figure can be viewed in the online issue, which is available at www.interscience.wiley.com.]

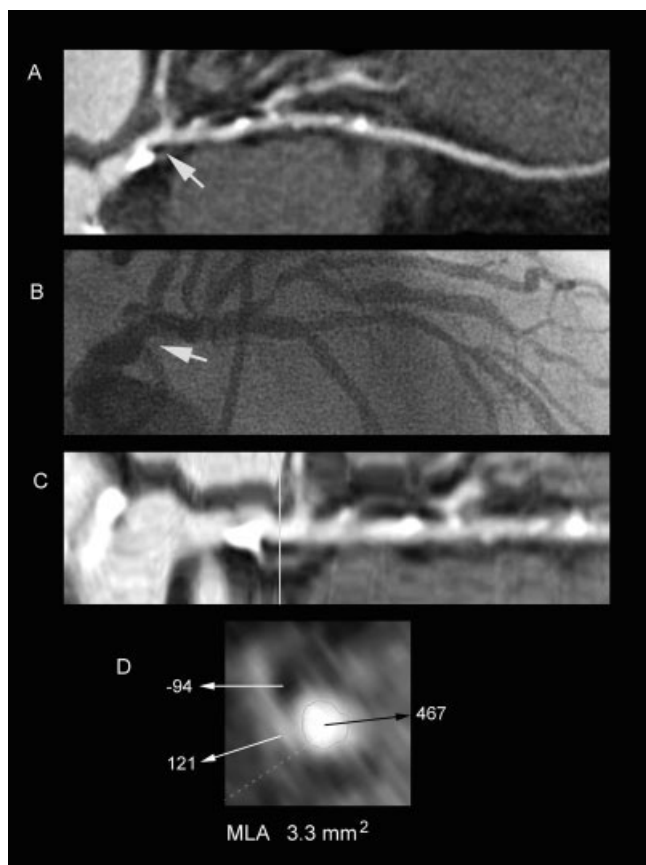


Fig. 11. CTA in an 82-year-old male with dyspnea revealed significant LM stenosis (A, arrow) much less apparent on CA (B, arrow). TIVA (D) of the straightened MPR (C) demonstrated a critically reduced MLA (3.3 mm^2), and a large low-density (-94 HU) lipid laden plaque adjacent to the lumen, consistent with a TCFA. CABG was performed. Abbreviations: CA, conventional angiography; CABG, coronary artery bypass grafting; CTA, computed tomographic angiography; HU, Hounsfield units; LM, left main; MLA, minimum luminal area; MPR, multiplanar reconstruction; TCFA, thin cap fibroatheroma; TIVA, tomographic intravascular analysis.

tion and may provide solutions, as may dual source imaging advances. Despite these limitations, CTA offers the best noninvasive hope for coronary plaque analysis; magnetic resonance angiography, while excellent for carotid and aortic plaque evaluation, is inadequate for the rapidly moving coronary circulation. Substantial IVUS correlated data supports the ability of CTA to reasonably assess plaque eccentricity, remodeling, volume, calcified and noncalcified plaque in both stable and unstable patients [22–29].

The noninvasive identification of the high-risk thin cap fibroatheroma (TCFA) [30,31] would provide a powerful tool for further investigation, particularly if the PROSPECT study confirms a convincing association of future clinical events with TCFAs identified by IVUS virtual histology analysis at the time of the ini-

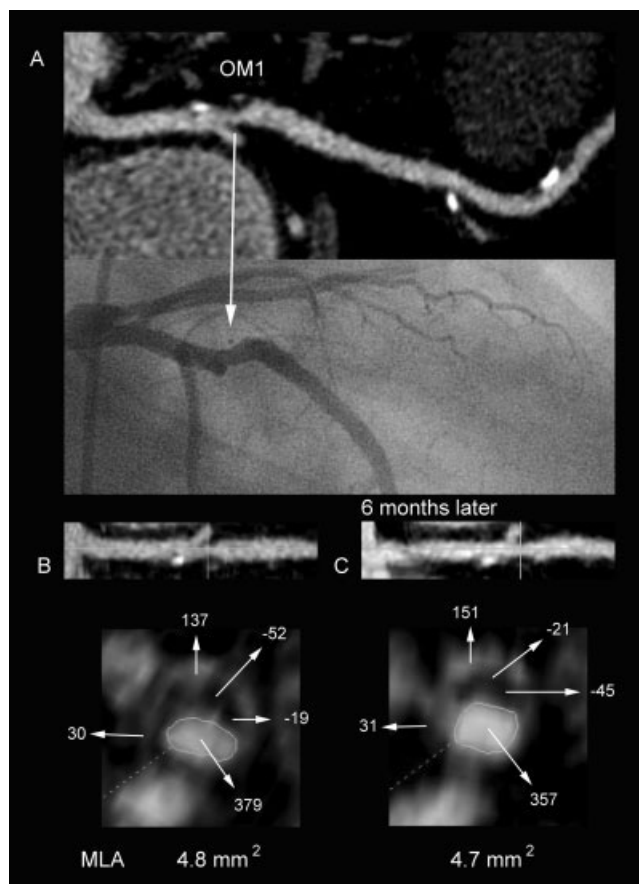


Fig. 12. A 62-year-old male with atypical chest pain underwent CTA (A) which demonstrated moderately severe ostial OM1 stenosis (arrow) that was not apparent on CA (B). TIVA of the straightened MPR (C) revealed a large low-density (-19 to -52 HU) lipid laden plaque adjacent to the lumen, consistent with a TCFA. However, the MLA was adequate (4.8 mm^2), and PCI was not performed. Six months later, chest pain recurred and CTA revealed no change in the plaque characteristics or MLA (D). Aggressive medical therapy was continued. Abbreviations: CA, catheter angiography; CTA, computed tomographic angiography; HU, Hounsfield units; MLA, minimum luminal area; MPR, multiplanar reconstruction; OM1, first obtuse marginal branch; PCI, percutaneous coronary intervention; TCFA, thin cap fibroatheroma; TIVA, tomographic intravascular analysis.

tial presentation with an acute coronary syndromes. In reality, TCFA may be diagnosed by CTA with a reasonable degree of certainty when a lipid core can be identified despite the above limitations. While there have been no studies correlating CTA defined TCFA with histology, the classic TCFA characteristics may be observed on CTA cross-sectional evaluation (Figs. 11–14): (1) focal (adjacent to non-TCFA); (2) lipid core $\geq 10\%$; (3) direct contact with the lumen; (4) percent area obstruction $\geq 40\%$. The impact on PCI is hypothetical at this point. If early PCI for nonobstructive TCFA containing lesions proves beneficial, CTA

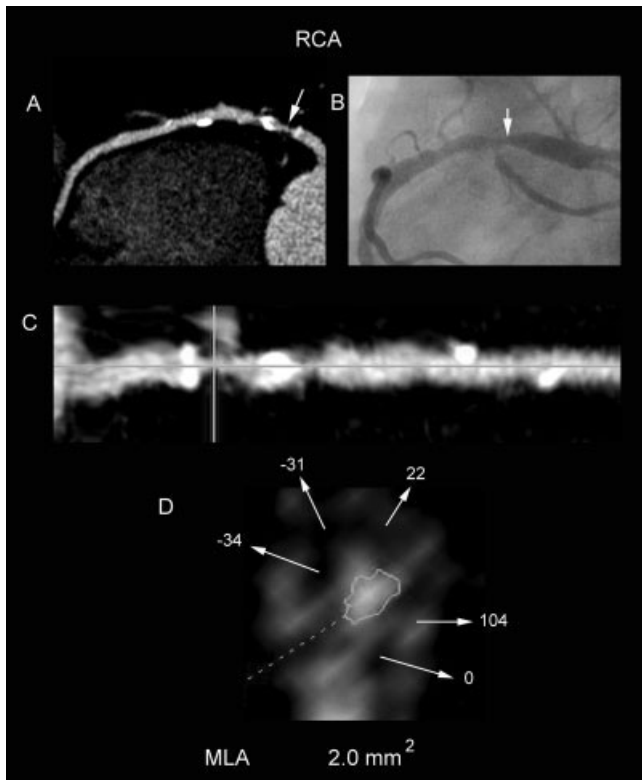


Fig. 13. A 61-year-old male presented with substernal burning. CTA revealed severe proximal RCA stenosis (A), confirmed by CA (B). TIVA (D) of the straightened MPR (C) demonstrated critically reduced MLA (2.0 mm^2) and a large low-density (-34 HU) lipid laden plaque adjacent to the lumen, consistent with a TCFA. PCI was performed. Abbreviations: CA, conventional angiography; CTA, computed tomographic angiography; HU, Hounsfield units; MLA, minimum luminal area; MPR, multiplanar reconstruction; PCI, percutaneous coronary intervention; RCA, right coronary artery; TCFA, thin cap fibroatheroma; TIVA, tomographic intravascular analysis.

may provide an ideal noninvasive identification of the high-risk patient; i.e., the patient with either single or multiple proximal TCFAs.

More readily identifiable high-risk characteristics are plaques with positive remodeling [32] and rupture (Fig. 15) [33], both of which are associated with a higher risk of acute coronary events. Data justifying PCI for nonobstructive lesions with these characteristics in the asymptomatic patient is still lacking, but the ability to identify them noninvasively provides a promising research avenue. Aggressive medical intervention is clearly appropriate for patients demonstrating high-risk plaque characteristics.

POSTCATHETERIZATION DECISIONS

CTA may be the only available tool to resolve questions left unanswered by CA, impacting directly on

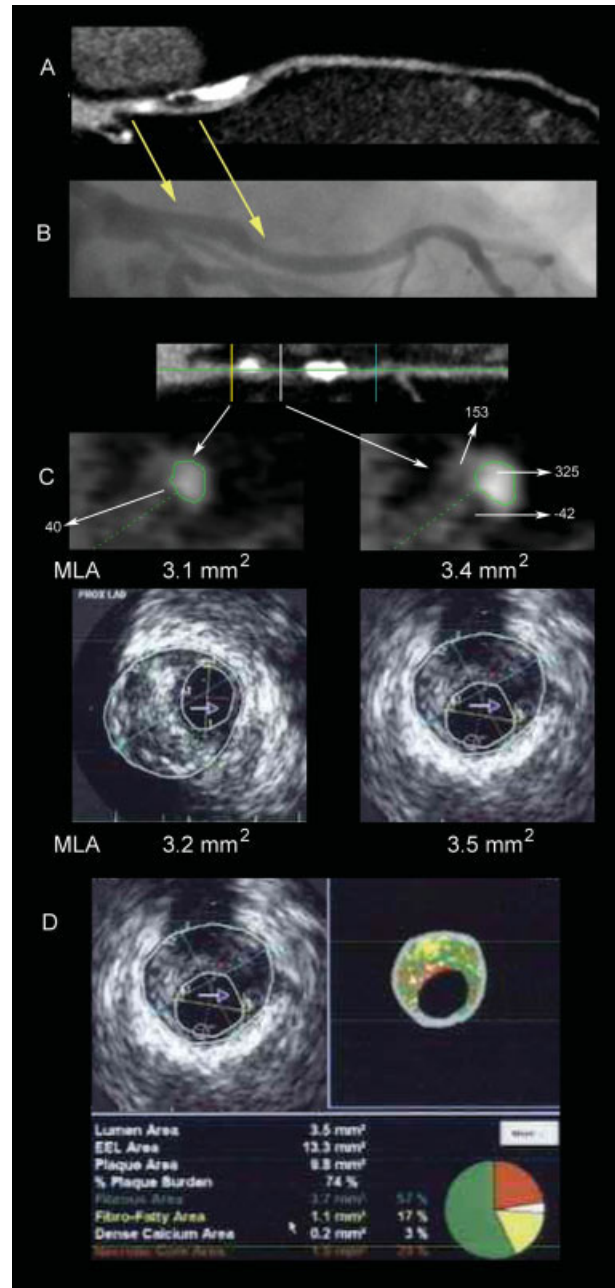


Fig. 14. An asymptomatic 71-year-old male with peripheral vascular disease underwent CTA which revealed significant ostial and proximal LAD disease (arrows). The ostial lesion was less impressive on CA (B). TIVA of the straightened MPR (C) revealed significantly equally reduced MLA at both sites (upper right and right), confirmed by IVUS (lower left and right). PCI of both lesions was performed. In the proximal LAD (upper right), a moderate sized low-density (-42 HU) lipid laden plaque was noted, consistent with a TCFA. Virtual histology of the proximal LAD lesion (D) revealed a large necrotic core (23% of total plaque volume), confirming the presence of a TCFA. Abbreviations: CA, conventional angiography; CTA, computed tomographic angiography; HU, Hounsfield units; LAD, left anterior descending; MLA, minimum luminal area; MPR, multiplanar reconstruction; TCFA, thin cap fibroatheroma; TIVA, tomographic intravascular analysis. [Color figure can be viewed in the online issue, which is available at www.interscience.wiley.com.]

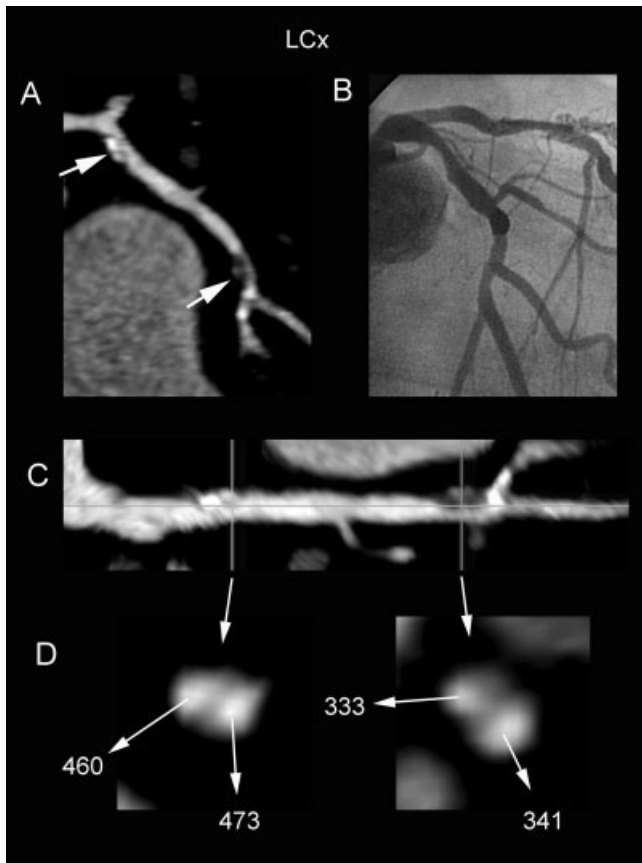


Fig. 15. A 52-year-old male with prior PCI underwent CTA (A) after presenting with recurrent chest pain. In the proximal LCx (arrow), a complex plaque was noted, containing calcified plaque and a second component extrinsic to the lumen, with density similar to contrast. In the mid LCx, a similar extraluminal density was noted (arrow). CA performed 2 weeks later (B) did not reveal these findings and the mid LCx stenosis was not apparent. TIVA (D) of the straightened MPR (C) confirmed the extraluminal densities to be similar to contrast, consistent with plaque rupture at both sites. Abbreviations: CA, conventional angiography; CTA, computed tomographic angiography; LCx, left circumflex; MPR, multiplanar reconstruction; PCI, percutaneous coronary intervention; TIVA, tomographic intravascular analysis.

PCI in situations where complete delineation of coronary or graft anatomy is crucial to decision making.

Failure of Image Acquisition

The most common situations are inability to selectively cannulate a vessel, including anomalous coronary arteries (Fig. 16), native coronaries originating from an aneurysmally dilated aortic root, right internal mammary grafts, and vein grafts originating from unanticipated aortic locations. Occasionally, severe pressure damping of the left main or right coronary artery may preclude safe contrast injection. CTA will invariably provide the necessary information.

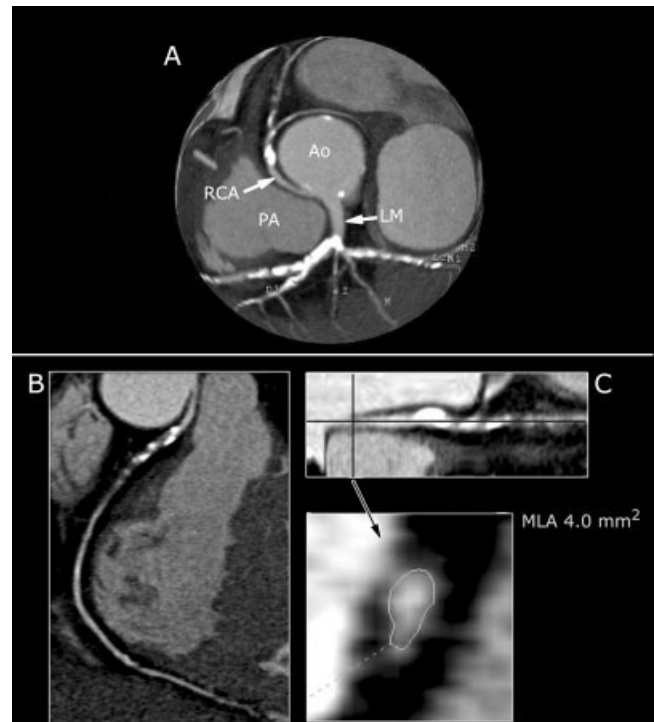


Fig. 16. In a 56-year-old male with angina, the anomalous right coronary artery could not be selectively cannulated. CTA revealed the vessel arising from the left coronary sinus, passing anteriorly between the aorta and pulmonary artery as shown in the maximum intensity pixel globe (A). The curved MPR displays ostial stenosis and total occlusion of the mid-portion (B). TIVA of the straightened MPR (C) demonstrated an MLA of 4.0 mm². CABG was performed because of the accompanying severe mid LAD stenosis. If CTA had not revealed severe RCA disease, PCI of the LAD would have been chosen. Abbreviations: CA, CABG= coronary artery bypass grafting; CTA, computed tomographic angiography; LAD, left anterior descending; MLA, minimum luminal area; MPR, multiplanar reconstruction; PCI, percutaneous coronary intervention; TIVA, tomographic intravascular analysis.

Requirement for Additional Information

Even after successful selective CA, there may be unresolved questions for which CTA is invaluable. These include differentiating ostial disease from coronary spasm unrelieved by intracoronary nitroglycerin, determining the potentially malignant anterior versus the benign posterior course of anomalous coronaries, establishing the relationship of mammary and vein grafts to the sternum to avoid transection during repeat bypass surgery, distinguishing venous bypass aneurysms from pseudoaneurysms, and demonstrating the path and length of CTOs.

STRUCTURAL HEART DISEASE

Percutaneous closure of atrial and ventricular septal defects (Fig. 17) is already being facilitated by incor-

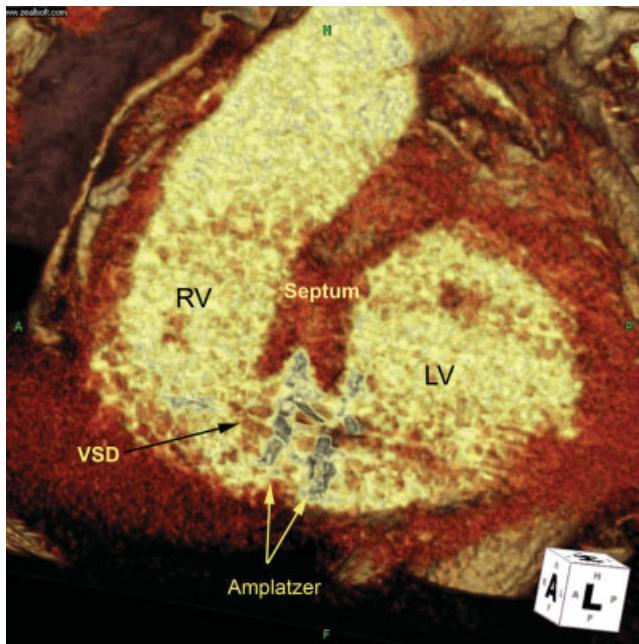


Fig. 17. A 63-year-old female presented with an acute anterior MI; 4 days later cardiogenic shock developed and a distal VSD was discovered and surgically patched. Acute symptoms recurred 1 week later accompanied by dehiscence of the patch. CTA was performed, and the VSD was closed with a post-MI-VSD Amplatzer with CTA guidance and confirmation of proper device placement (Courtesy of Dr. Carlos Ruiz). Abbreviations: CTA, computed tomographic angiography; LV, left ventricle; MI, myocardial infarction; RV, right ventricle; VSD, ventricular septal defect. [Color figure can be viewed in the online issue, which is available at www.interscience.wiley.com.]

poration of the structural data provided by CTA directly into the catheterization laboratory. Percutaneous aortic valve replacements will also benefit by precise measures of annular size and structure, and the three-dimensional relationships of the valvular apparatus to the septum, ventricle, and aorta.

CONCLUSIONS

The fact that CTA will significantly alter the practice of PCI is abundantly clear; it is still in its relative infancy, with forthcoming technologic advances likely to accelerate the pace of change. The prerequisite human ingredient is a change in mind set, an acknowledgement that the traditional reliance on catheter angiography is limiting, despite the decades of data accumulated in the catheterization laboratory. Had IVUS been available from the very beginning of angiography, there is little doubt that it would have been the gold standard. CTA provides the opportunity to incorporate the unique insights offered by IVUS into a universally available noninvasive tool which can now be

brought directly into the catheterization laboratory. The likely outcome is transformation of the catheterization laboratory into a streamlined interventional suite, utilizing on-line CTA data in an interactive format. "How did we ever do without it?" will be a common refrain as awareness of the capabilities of CTA exponentially expands.

REFERENCES

1. Fleischmann KE, Hunink MG, Kuntz KM, Douglas PS. Exercise echocardiography or exercise SPECT imaging? A meta-analysis of diagnostic test performance. *JAMA* 1998;280:913–920.
2. Hecht HS, Roubin G. Usefulness of computed tomographic angiography guided percutaneous coronary intervention. *Am J Cardiol* 2007;99:871–875.
3. Lima RSL, Watson DD, Goode AR, et al. Incremental value of combined perfusion and function over perfusion alone by gated SPECT myocardial perfusion imaging for detection of severe three-vessel coronary artery disease. *J Am Coll Cardiol* 2003;42:64–70.
4. Berman DS, Kang X, Slomka PJ, et al. Underestimation of extent of ischemia by gated spect myocardial perfusion imaging in patients with left brain coronary disease. *J Nucl Cardiol* 2007;14:521–528.
5. Abizaid AS, Mintz GS, Mehran R, et al. Long-term follow-up after percutaneous transluminal coronary angioplasty was not performed based on intravascular ultrasound findings: Importance of lumen dimensions. *Circulation* 1999;100:256–261.
6. Takagi A, Tsurumi Y, Ishii Y, et al. Clinical potential of intravascular ultrasound for physiological assessment of coronary stenosis relationship between quantitative ultrasound tomography and pressure-derived fractional flow reserve. *Circulation* 1999;100:250–255.
7. Nishioka T, Amanullah AM, Luo H, et al. Clinical validation of intravascular ultrasound imaging for assessment of coronary stenosis severity. Comparison with stress myocardial perfusion imaging. *J Am Coll Cardiol* 1999;33:1870–1878.
8. Tobis J, Azarbal B, Slavin L. Assessment of intermediate severity coronary lesions in the catheterization laboratory. *J Am Coll Cardiol* 2007;49:839–848.
9. Bech GJW, Bruyne BD, Pijls NHJ, et al. Fractional flow reserve to determine the appropriateness of angioplasty in moderate coronary stenosis. A randomized trial. *Circulation* 2001;103:2928–2934.
10. Ragosta M, Bishop AH, Lipson LC, et al. Comparison between angiography and fractional flow reserve versus single-photon emission computed tomographic myocardial perfusion imaging for determining lesion significance in patients with multivessel coronary disease. *Am J Cardiol* 2007;99:896–902.
11. Christou MAC, Siontis GCM, Katritsis DG, et al. Meta-analysis of fractional flow reserve versus quantitative coronary angiography and noninvasive imaging for evaluation of myocardial ischemia. *Am J Cardiol* 2007;99:450–456.
12. Achenbach S, Ropers D, Hoffmann U, et al. Assessment of coronary remodeling in stenotic and nonstenotic coronary atherosclerotic lesions by multidetector spiral computed tomography. *J Am Coll Cardiol* 2004;43:842–847.
13. Moselewski F, Ropers D, Pohle K, et al. Measurement of cross-sectional coronary atherosclerotic plaque and vessel areas by 16-slice multi-detector CT: Comparison to IVUS. *Am J Cardiol* 2004;94:1294–1297.

14. Caussin C, Larchez C, Ghostine S, et al. Comparison of coronary minimal lumen area quantification by sixty-four-slice computed tomography versus intravascular ultrasound for intermediate stenosis. *Am J Cardiol* 2006;98:871–876.
15. Rixe J, Achenbach S, Ropers D, et al. Assessment of coronary artery stent restenosis by 64-slice multi-detector computed tomography. *Eur Heart J* 2006;27:2567–2572.
16. Cademartiri F, Schuijf JD, Pugliese F, et al. Usefulness of 64-slice multislice computed tomography coronary angiography to assess in-stent restenosis. *J Am Coll Cardiol* 2007;49:2204–2210.
17. Ehara M, Kawai M, Surmely J, et al. Diagnostic accuracy of coronary in-stent restenosis using 64-slice computed tomography. *J Am Coll Cardiol* 2007;49:951–959.
18. Hecht HS, Zaric M, Jelmin V, et al. Detection of in-stent restenosis by 64-detector computed tomographic angiography. *Am J Cardiol*, in press.
19. Hendel RC, Patel MR, Kramer C, et al. ACCF/ACR/SCCT/SCMR/ASNC/NASCI/SCAI/SIR 2006 appropriateness criteria for cardiac computed tomography and cardiac magnetic resonance imaging: A report of the American College of Cardiology Foundation Quality Strategic Directions Committee Appropriateness Criteria Working Group, American College of Radiology, Society of Cardiovascular Computed Tomography, Society for Cardiovascular Magnetic Resonance, American Society of Nuclear Cardiology, North American Society for Cardiac Imaging, Society for Cardiovascular and Interventions, and Society of Interventional Radiology. *J Am Coll Cardiol* 2006;48:1475–1497.
20. Holmes DR, Kereiakes DJ, Laskey WK, et al. Thrombosis and drug-eluting stents: An objective appraisal. *J Am Coll Cardiol* 2007;50:109–118.
21. Mollet NR, Hoye A, Lemos PA, et al. Value of preprocedure multislice computed tomographic coronary angiography to predict the outcome of percutaneous recanalization of chronic total occlusions. *Am J Cardiol* 2005;95:240–243.
22. Schroeder S, Kopp AF, Baumbach A, et al. Noninvasive detection and evaluation of atherosclerotic coronary plaques with multislice computed tomography. *J Am Coll Cardiol* 2001;37:1430–1435.
23. Caussin C, Ohanessian A, Lancelin B, et al. Coronary plaque burden detected by multislice computed tomography after acute myocardial infarction with near-normal coronary arteries by angiography. *Am J Cardiol* 2003;92:849–842.
24. Caussin C, Ohanessian A, Ghostine S, et al. Characterization of vulnerable nonstenotic plaque with 16-slice computed tomography compared with intravascular ultrasound. *Am J Cardiol* 2004;94:99–104.
25. Leber AW, Knez A, Becker A, et al. Accuracy of multidetector spiral computed tomography in identifying and differentiating the composition of coronary atherosclerotic plaques: A comparative study with intracoronary ultrasound. *J Am Coll Cardiol* 2004;43:1241–1247.
26. Achenbach S, Moselewski F, Ropers D, et al. Detection of calcified and noncalcified coronary atherosclerotic plaque by contrast enhanced, submillimeter multidetector spiral computed tomography: A segment-based comparison with intravascular ultrasound. *Circulation* 2004;109:14–17.
27. Hausleiter J, Meyer T, Hadamitzky M, et al. Prevalence of noncalcified coronary plaques by 64-slice computed tomography in patients with an intermediate risk for significant coronary artery disease. *J Am Coll Cardiol* 2006;48:312–318.
28. Hoffmann U, Moselewski F, Nieman K, et al. Noninvasive assessment of plaque morphology and composition in culprit and stable lesions in acute coronary syndrome and stable lesions in stable angina by multidetector computed tomography. *J Am Coll Cardiol* 2006;47:1655–1662.
29. Leber AW, Becker A, Knez A, et al. Accuracy of 64-slice computed tomography to classify and quantify plaque volumes in the proximal coronary system. A comparative study using intravascular ultrasound. *J Am Coll Cardiol* 2006;47:672–677.
30. Kolodgie FD, Burke AP, Farb A, et al. The thin-fibrous cap fibroatheroma: A type of vulnerable plaque: The major precursor lesion to acute coronary syndromes. *Curr Opin Cardiol* 2001;16:285–292.
31. Virmani R, Kolodgie FD, Burke AP, Farb A, Schwartz SM. Lessons from sudden coronary death: A comprehensive morphological classification scheme for atherosclerotic lesions. *Arterioscler Thromb Vasc Biol* 2000;20:1262–1275.
32. Varnava AM, Mills PG, Davies MJ. Relationship between coronary artery remodeling and plaque vulnerability. *Circulation* 2002;105:939–943.
33. von Birgelen C, Klinkhart W, Mintz GS, et al. Plaque distribution and vascular remodeling of ruptured and nonruptured coronary plaques in the same vessel: An intravascular ultrasound study in vivo. *J Am Coll Cardiol* 2001;37:1864–1870.